ADVANCED FUNCTIONAL MATERIALS
www.afm-journal.de

www.MaterialsViews.com

Thermally Stable, Biocompatible, and Flexible Organic Field-Effect Transistors and Their Application in Temperature Sensing Arrays for Artificial Skin

Xiaohan Wu, Yan Ma, Guoqian Zhang, Yingli Chu, Juan Du, Yin Zhang, Zhuo Li, Yourong Duan, Zhongyong Fan, and Jia Huang**

Application of degradable organic electronics based on biomaterials, such as polylactic-*co*-glycolic acid and polylactide (PLA), is severely limited by their low thermal stability. Here, a highly thermally stable organic transistor is demonstrated by applying a three-arm stereocomplex PLA (tascPLA) as dielectric and substrate materials. The resulting flexible transistors are stable up to 200 °C, while devices based on traditional PLA are damaged at 100 °C. Furthermore, charge- trapping effect induced by polar groups of the dielectric is also utilized to significantly enhance the temperature sensitivity of the electronic devices. Skin-like temperature sensor array is successfully demonstrated based on such transistors, which also exhibited good biocompatibility in cytotoxicity measurement. By presenting combined advantages of transparency, flexibility, thermal stability, temperature sensitivity, degradability, and biocompatibility, these organic transistors thus possess a broad applicability such as environment friendly electronics, implantable medical devices, and artificial skin.

1. Introduction

Degradable and environmentally friendly electronics based on biomaterials and organic semiconductors are attracting intensive research and commercial interest because they enable a range of biocompatible devices for consumer electronics, such as those used for biomonitoring and artificial skin.[1–3] Controlled device degradation is also important to help eliminate the growing problem of "electronic pollution" in the environment.[1,4–7] For these reasons, biodegradable polymers, such as polylactic-*co*-glycolic acid (PLGA) and polylactide (PLA), are being explored for fabrication of the aforesaid organic electronics.[1] PLA exhibits especially good biocompatibility and degradability, which has allowed it to be approved for use by the United States Food and Drug Administration (FDA).[8–11] However, thermal instability is a major issue of biomaterial-based electronics due to the typically low melting temperature of these materials, which makes such devices vulnerable to damage when annealed or sterilized as required during device fabrication or operation.[1,5]

Moreover, organic electronics are being broadly applied as sensors thanks to their cost efficiency and portability.[12–17] In addition to the inherent sensitivity of organic semiconductors, device configuration is another approach to provide increased sensing capability. For instance, microstructured polydimethylsiloxane films were integrated into organic field-effect transistors (OFETs) as the dielectric layer to provide high-pressure sensitivity.[18,19] Organic semiconductors often show temperature-dependent intrinsic field-effect mobility at temperatures ranging from 4 k to 300 k, but display very limited thermal sensitivity beyond room temperature, which would be of more practical use.[20,21] To overcome this limitation, the introduction of polar groups within the dielectric layer can provide an interfacial interaction with charge carriers of the organic semiconductor layer in a manner that can be influenced by changes in the environment, such as temperature, which can be exploited for thermal sensing. Therefore, incorporating a biodegradable polymer, such as PLA, containing strong polar groups in the

Dr. X. Wu, G. Zhang, Y. Chu, J. Du, Dr. Y. Zhang, Prof. J. Huang
School of Materials Science and Engineering
Tongji University
Shanghai 201804, P.R. China
Key Laboratory of Advanced Civil Engineering Materials
Tongji University
Ministry of Education
Shanghai 201804, P.R. China
E-mail: huangjia@tongji.edu.cn
Y. Ma, Prof. Z. Fan
Department of Materials Science
Fudan University
Shanghai 200433, P.R. China
E-mail: zyfan@fudan.edu.cn
Dr. Z. Li
State Key Laboratory of Pollution
Control and Resource Reuse
College of Environmental Science and Engineering
Tongji University
Shanghai 200092, P.R. China
Prof. Y. Duan
Shanghai Cancer Institute
Renji Hospital, School of Medicine
Shanghai Jiao Tong University
Shanghai 200032, P.R. China

DOI: 10.1002/adfm.201404535

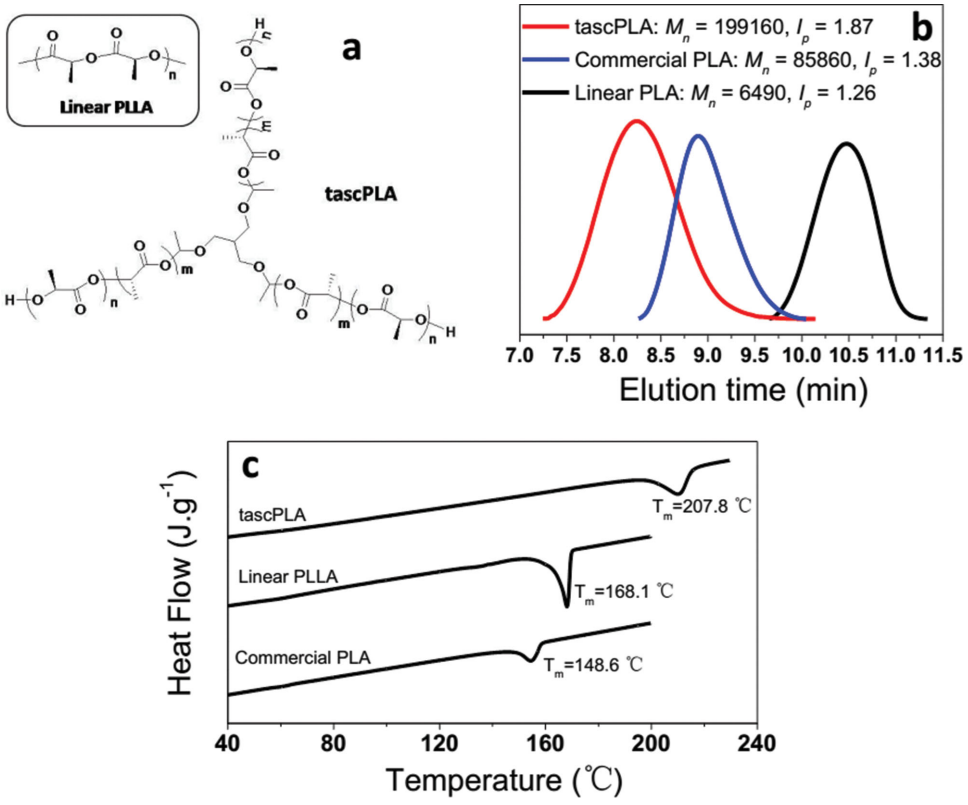

Figure 1. Molecular characterization and thermal properties of different PLA: a) chemical structures of tascPLA and linear PLLA, b) GPC curves of tascPLA (left), linear PLLA (right) and commercial PLA (middle) and c) DSC curves of the three polymers for the first heating cycle.

polymer chain is considered as a new dielectric layer for OFETs to enhance thermal sensitivity of biocompatible devices beyond room temperature for thermal sensing applications.

In this work, we demonstrate a thermally stable biomaterial-based OFET by applying a three-arm stereocomplex PLA (tascPLA), that serves as the gate dielectric and substrate simultaneously. Various organic semiconductors, including both p-type dinaphtho[2,-b:2′,3′-f]-thieno[3,2-b]thiophene (DNTT), 5,5′-bis(4-n-hexylphenyl)-2,2′-bithiophene (6PTTP6), and n-type *N,N*-bis (3-(perfluoroctyl)propyl)-1,4,5,8-naphthalenetetracarboxylic acid diimide (8_3-NTCDI),[17,22,23] were used to fabricate the transistor channels. The resulting tascPLA–OFETs are stable up to 200 °C, while devices based on traditional PLA are generally damaged at 100 °C. The transistors also display good flexibility and operation even while bent around a radius of less than 800 µm. As we expected, the temperature sensitivity of the tascPLA–OFETs was significantly enhanced by utilizing polar group induced dielectric/semiconductor interfacial charge-trapping effect, without which the semiconductor materials alone display very limited temperature-dependent performance beyond room temperature. Cytotoxicity of the devices was also evaluated using cell co-cultures and 3-(4,5-dimethyl-thiazol-2-yl)-2,5-diphenyl-tetrazolium bromide (MTT) assays, demonstrating good biocompatibility. Skin-like temperature sensing was then realized by constructing an array of the tascPLA–OFETs, and further validated against thermal infrared imaging. By presenting combined advantages of transparency, flexibility, high thermal stability, temperature sensitivity, degradability, and biocompatibility, our transistors thus possess broad applicability for environmentally friendly electronics, implantable medical devices, and artificial skin.

2. Results and Discussion

2.1. Molecular Design and Synthesis of Thermally Stable PLA

PLA has been used as an environmentally friendly engineering and biomaterial because of its good mechanical properties and degradability.[24,25] Commercial PLA is typically obtained from natural plant sugars, which consists of mainly poly(L-lactic acid) (PLLA) with trace poly(D-lactic acid) (PDLA). The material exhibits a rather low-melting temperature (T_m) at less than 150 °C since the presence of trace PDLA disturbs crystallization of the PLLA. However, crystalline stereocomplex PLA (scPLA), consisting of similar amounts of PLLA and PDLA, is harder to break due to the interaction between the two configurations, and thus scPLA shows a higher T_m as compared to pure PLLA or PDLA.[26] A block copolymer chain with equal amounts of PLLA and PDLA was therefore considered for a biomaterial-based device to ensure that the PLA crystal structure consisted of mostly scPLA. Additionally, the interesting properties of multiarmed polymers, such as their improved processing and strong mechanical properties,[27] suggested such a molecular structure incorporating three arms and PLLA–PDLA block chains would be most advantageous for the proposed applications and was thus designed for our thermally stable PLA material (**Figure 1**a). Synthesis of the

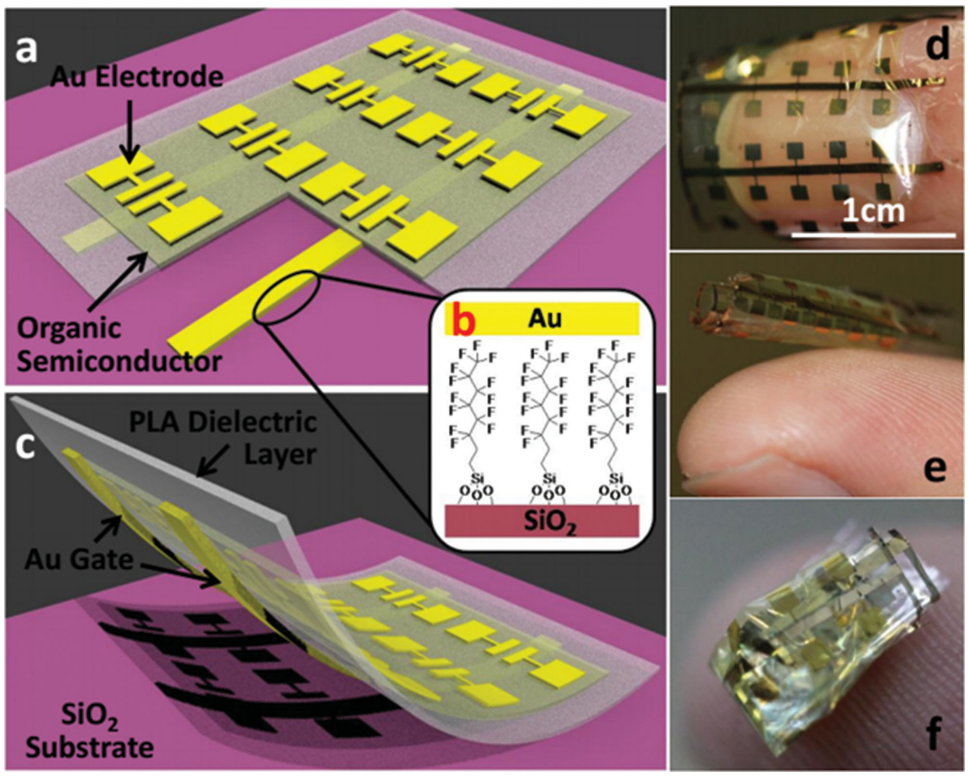

Figure 2. Schematic presentations of OFET device fabrication and images of the transparent and flexible OFETs: a) construction of the OFETs, b) release layer treatment of the Si template, C) OFETs peeling off from the Si template, d) image of the OFETs, e) crispation of the OFETs and f) multifolded OFETs.

tascPLA was realized according to the route depicted in Figure s1 (Supporting Information).[28] Three-arm PDLA was first obtained by ring-opening polymerization of D-lactide using a three-arm poly (propylene oxide) (PPO) as the initiator. Tin (II)-alkoxide groups (tin (II) octoate, SnOct) were used to end functionalize the three-arm PDLA, and the resulting prepolymer acted as an efficient initiator in further polymerization of L-lactide to yield high-molecular-weight (Mw) tascPLA. The final product was characterized by gel permeation chromatography (GPC) (Figure 1b), proton nuclear magnetic resonance (^{1}H NMR), ^{13}C NMR (Figure s2, Supporting Information), and spectropolarimetery. D-lactyl unit content of the tascPLA was 53.2%. A Mw of 160 000 g mol^{-1} for the tascPLA was calculated using ^{1}H NMR, indicating successful synthesis of the copolymer. It should be noted that the thermal properties of PLA as measured by differential scanning calorimetry (DSC) were not just dependent on its Mw. Commercial PLA has a much higher Mw but a lower T_m than the linear PLLA. Interestingly, the tascPLA's elaborate molecular structure exhibits the highest thermal properties, with a T_m of over 200 °C (Figure 1c, s2, Supporting Information).

2.2. OFETs Fabrication and Flexibility Measurements

The PLA-based transistor geometry and fabrication approach are illustrated in **Figure 2**. Gold gate electrodes were first evaporated onto silicon (Si) templates that were pretreated with a (tridecafluoro-1,1,2,2-tetrahydrooctyl)trichlorosilane (FOTS) self-assembled monolayer (SAM) as a release layer (Figure 2b).[29] 5 µm dielectric membranes that also served as the device substrate were then fabricated onto the gate electrodes by either spin-coating or dip-coating of the PLA solution. Both tascPLA and linear PLLA were used as the dielectric membranes. Organic semiconductors and gold drain/source electrodes were deposited onto the PLA layers by thermal evaporation. For some organic semiconductors (e.g., 8_3-NTCDI), elevated substrate temperature during the thermal evaporation process generates improved transistor performance.[22] However, the thermal instability of the linear PLLA limited the choice of substrate temperatures, thus all the organic semiconductors were evaporated with the substrate temperatures at less than 80 °C. The OFETs were easily peeled off from the Si templates due to the presence of the release layer (Figure 2c), which allowed the Si wafers to be reused as templates. The OFETs show great flexibility (Figure 2d) as they can be naturally curled (Figure 2e) and reversibly multi-folded (Figure 2f). The great mechanical flexibility enables a wide range of interesting applications such as wearable electronics.[30,31]

To demonstrate the applicability of the PLA dielectric in organic electronics, several organic semiconductors, including both n-type (8_3-NTCDI) and p-type (6PTTP6, DNTT), were used in the OFETs.[17,22,23] The performance of the obtained OFETs was evaluated using a Keithley 4200 Semiconductor Parameter Analyzer. All the OFETs exhibited good transistor characteristics, as shown in **Figure 3**a–c, displaying obvious linear and saturation regimes. The flexibility of the OFETs was

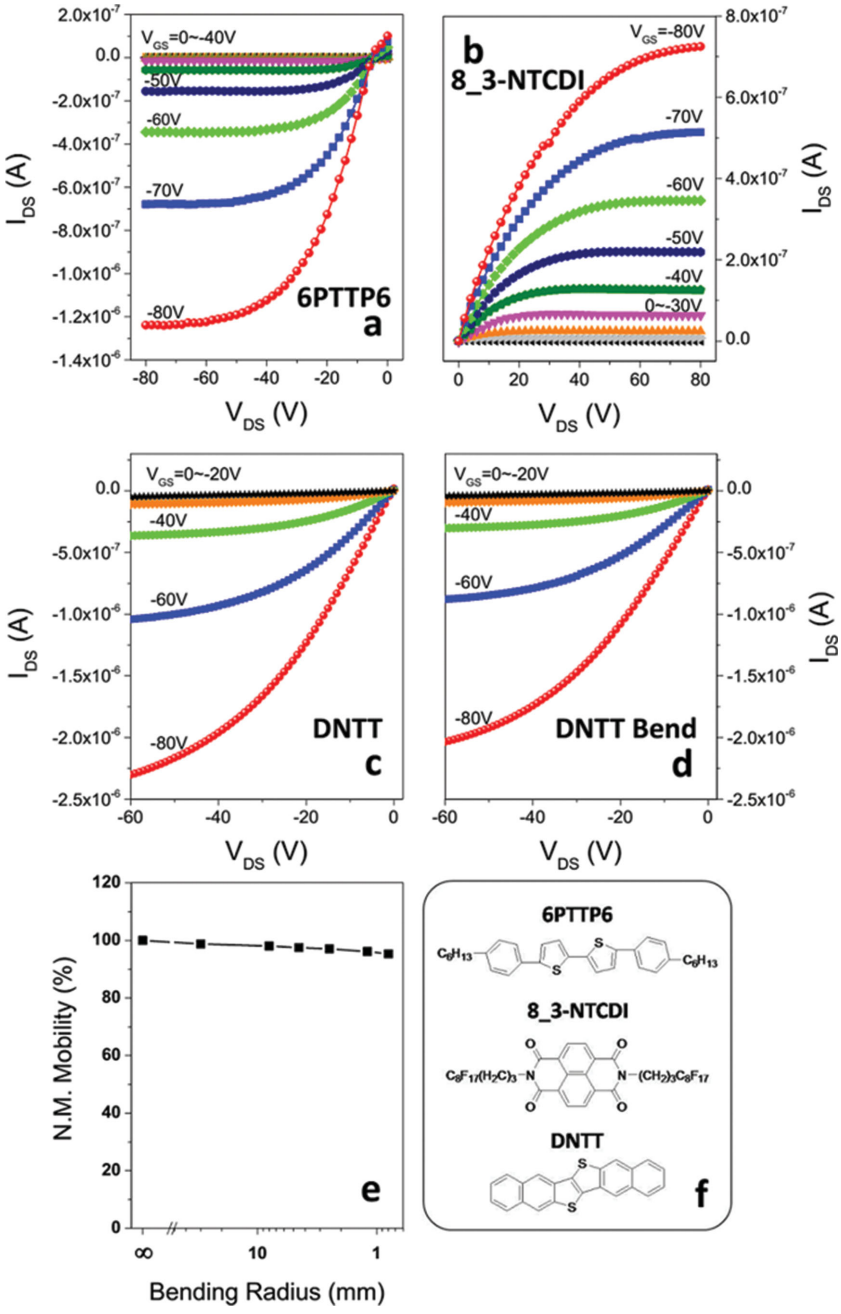

Figure 3. Electrical performance and flexibility of the tascPLA–OFETs with different organic semiconductors: I_{DS}–V_{DS} characteristics of the OFET with a) 6PTTP6, b) 8_3-NTCDI, c) DNTT, d) DNTT while the tascPLA–OFET is bent around a radius of 800 µm, e) mobility variation of the DNTT-tascPLA–OFET at different bending radii, normalized to the initial mobility measured at the flat state (bending radius of ∞ indicates the OFET is flat) and f) molecular structures of the three organic semiconductors.

further demonstrated by measuring their electrical properties while wrapped around cylindrical rods with a series of radii.[32] I_{DS}–V_{DS} curves of the DNTT-tascPLA-OFET were measured for both flat devices (Figure 3c) and those bent around an 800 µm radius (Figure 3d). Both configurations exhibited good transistor characteristics, and the I_{DS} changed from −2.25 to −2.05 µA (V_{DS} = −60 V, V_{GS} = −80 V). The mobility variation of the OFET for flat and bent configurations at a radius ranging from 30 to 0.8 mm was obtained by measuring the transfer characteristic curves to determine that only a 4.7% decrease in mobility was observed (Figure 3e). It should be noted that a radius of 800 µm is not the bending limitation of our OFETs, rather the comparable electrical performance of the device whether kept flat or bent around an 800 µm radius indicates that the flexibility of the OFETs is good enough for most application requirements.[30]

2.3. Thermal Stability and Sensitivity

Thermal stability of the OFETs was evaluated by measuring their electronic performance at temperatures varying from room temperature to near the T_m of tascPLA (200 °C). The DNTT-tascPLA-OFETs maintained good transistor characteristics from room temperature to 200 °C (**Figure 4**a,d). In contrast, the output curves of the DNTT-linear PLLA-OFETs were disordered at less than 100 °C (Figure 4e,f), and then completely damaged at beyond 100 °C. This sharp contrast between the two kinds of OFETs indicates that the thermal stability of the biomaterial-based electronic is drastically improved by applying the tascPLA. By introducing biomaterials into organic electronics, devices displaying degradability and biocompatibility can be realized. However, thermal stability of such electronics is limited by the biomaterial additives.[1] PLA inherently exhibits better thermal stability compared to other biodegradable polymers such as PLGA and polycaprolactone (PCL), and was used here in the organic electronic devices.[11,25] Commercially available PLA presents a relatively low melting point (<150 °C), and thus was not applied in the OFETs. Linear PLLA exhibits higher melting temperature than the commercially PLA, but fabrication and application temperatures of linear PLLA-OFETs are still limited. For example, using an annealing temperature of over 100 °C during the thermal evaporation step could ruin the linear PLLA films by causing them to become brittle. Here, we demonstrate that the tascPLA has a melting point beyond 200 °C thanks to its multiarmed and scPLA crystal structure. OFETs based on the tascPLA can thus possess relatively comprehensive advantages.

The thermal sensitivity of the organic semiconductors alone is limited beyond room temperature. However, by taking advantage of the polar group induced charge-trapping effect, OFETs based on all the above-listed organic semiconductors can be provided with significantly enhanced thermal sensitivity. For

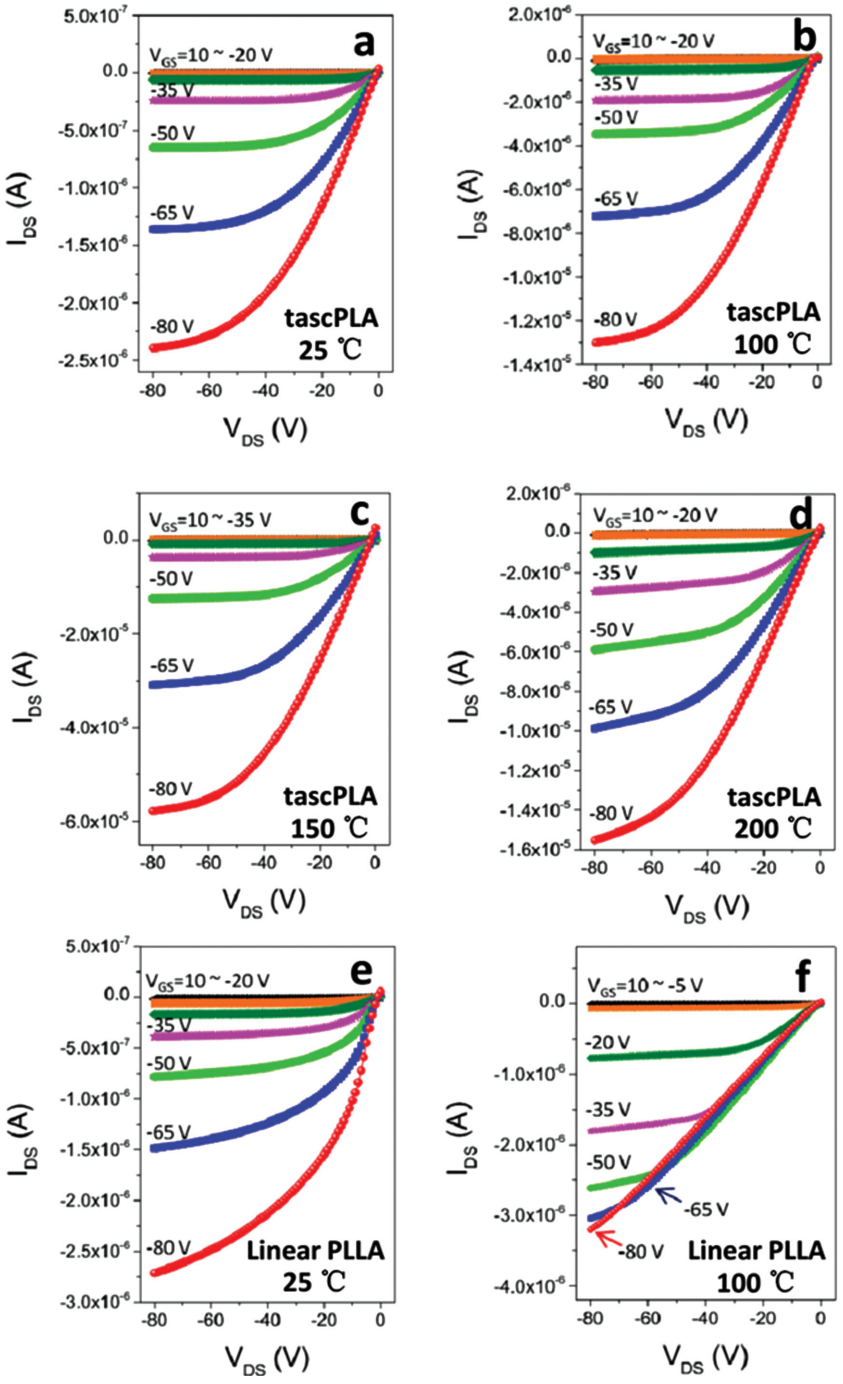

Figure 4. Thermal stability of the DNTT-tascPLA–OFET as compared with DNTT-linear PLLA-OFET: I_{DS}–V_{DS} characteristics of the DNTT-tascPLA-OFET at a) room temperature, b) 100 °C, c) 150 °C, and d) 200 °C and that of DNTT-linear PLLA-OFET at e) room temperature and f) 100 °C.

example, transfer characteristics of the tascPLA–OFET composed of the DNTT semiconductor at temperatures ranging from 25 °C to 150 °C are shown in **Figure 5**a. The I_{DS} of the device improves from 2.13 to 37.8 μA as the temperature increases from room temperature to 150 °C (V_{DS} = −60 V, V_{GS} = −80 V). Similar behaviors were also found for the tascPLA–OFETs fabricated with other semiconductors including p-type 6PTTP6 and n-type 8_3-NTCDI (Figure s3, Supporting Information). This thermal sensitivity behavior of the DNTT-tascPLA-OFET was further demonstrated by showing an intensive variation of I_{DS} against temperature ranging from –25 °C to 150 °C, as compared to the results obtained from DNTT–OFET made with a control silicon dioxide (SiO_2) dielectric (Figure 5b). The I_{DS} of tascPLA–OFET shows a continuous rise, while that of SiO_2–OFET remains relatively stable, indicating that the temperature-sensitive behavior is generated by the semiconductor/dielectric interfacial interaction. Stability of the thermally sensitive behavior was demonstrated through a repeated wave variation of temperature from 25 °C to 100 °C, showing a corresponding wave variation in the I_{DS} of the DNTT-tascPLA-OFET (Figure 5c). The tascPLA–OFETs were also held at 100 °C for several hours, and its I_{DS} exhibited slight changes (Figure 5d). These results indicate that the thermal sensitivity is both reliable and reproducible, making our tascPLA–OFETs applicable for temperature sensors.[33]

The trapping effect has been generally considered a problem for organic electronics, but here subtly applied in this work to enhance thermal sensitivity of the OFETs. The mechanism of the polar-group-induced thermal sensitivity can be described on the basis of the multiple trap and release (MTR) model.[20,34–37] Specifically, polar groups in the PLA layer (i.e., carbonyl functionalities) induce multiple traps with different energy levels at the semiconductor and dielectric interface. The deep traps with high energy levels can capture charge carriers and thus decrease the carrier density in the conduction channel. The shallow traps with relatively low energy levels can reduce the rate of charge carrier transportation by temporarily trapping the carriers. During energy uptake from heat at elevated temperature conditions, the carriers can be released from the deep traps. The rate of charge carrier transportation can also be increased since the average capture time by shallow traps is shortened. The charge carrier density and transportation rate at the interface dominate the threshold voltage (V_{th}) and mobility of the OFET, respectively.[34,36,37] Therefore, our tascPLA–OFETs exhibit reduced absolute V_{th} (e.g., from 37.5 to 0.36 V for DNTT-tascPLA-OFET) and increased mobility (e.g., from 0.15 to 0.58 $cm^2V^{-1}s^{-1}$ for DNTT-tascPLA-OFET) at elevated temperatures for all the studied organic semiconductors (Figure 5e,f, s3c,d, Supporting Information). Other factors

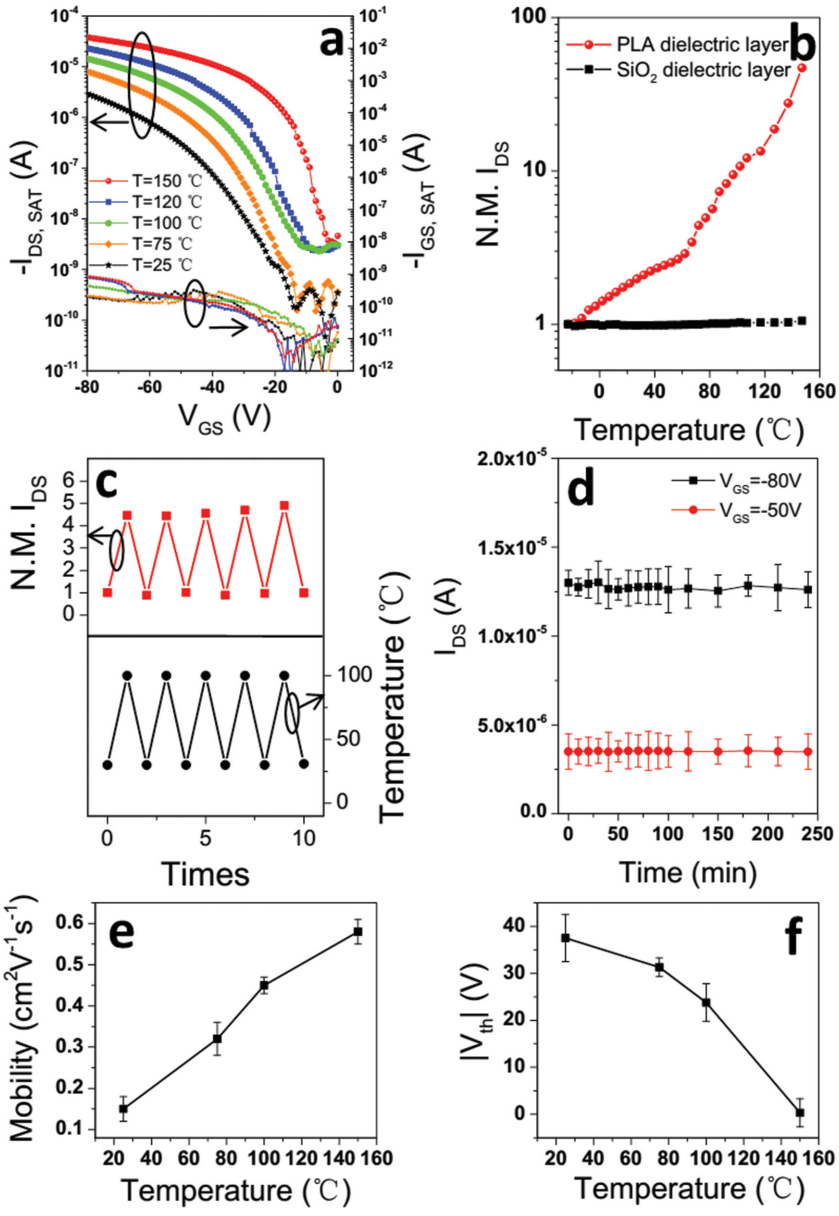

Figure 5. Temperature sensitivity of the tascPLA–OFETs: a) transfer characteristics at different temperatures of DNTT-tascPLA-OFET (V_{DS} = –60 V), the thin lines are corresponding gate leakages, b) I_{DS} variations of the OFETs with tascPLA or SiO_2 dielectric layers at different temperatures, normalized to the initial I_{DS} measured at –25 °C (V_{DS} = –60 V, V_{GS} = –60 V), c) I_{DS} variation of the DNTT-tascPLA-OFET along with repeated temperature changes between 25 °C and 100 °C, normalized to the initial I_{DS} measured at 25 °C, d) I_{DS} variation of the tascPLA–OFETs holding at 100 °C as a function of time (V_{DS} = –80 V), e) mobility, and f) threshold voltage variation of the DNTT-tascPLA-OFETs. Error bars in d, e, and f represent standard errors from 20 tascPLA–OFETs.

were also considered as possible reasons for the thermally sensitive behavior, such as intrinsic mobility changes of the organic semiconductors and capacitance changes of the PLA film. OFETs of DNTT deposited on Si/SiO_2 gate/dielectric were measured by the semiconductor parameter analyzer at temperatures ranging from –25 °C to 150 °C. The drain-source current and mobility of the OFET change slightly (Figure 5b), implying the intrinsic mobility of DNTT changes slightly in this temperature range. Variation of PLA layer capacitance is also evaluated and presented limited change (Figure s4, Supporting Information). The above findings indicate that the polar-group-induced MTR effect is the main mechanism of the high thermal sensitivity of our OFETs as we proposed. The strategy of utilizing the polar-group-induced semiconductor/dielectric interfacial charge-trapping effect, requiring only a very simple fabrication process, can be extensively applied to various organic semiconductors and electronics to significantly enhance their thermally sensitivity.

2.4. Biocompatibility

Biocompatibility is a basic requirement for materials and devices with potential biomedical applications.[11] PLA has good biocompatibility and has been approved by the FDA as a result.[9,10] However, the biocompatibility of biomaterial-based OFETs, which also contain organic semiconductors and metal electrodes, remains unknown. Cell co-cultures and MTT assays were employed to study the cytotoxicity of the tascPLA–OFETs.[11,38] The OFETs with 8_3-NTCDI semiconductor layers were immersed into a solution of L929 cells for co-culture measurements. After 4 days of incubation, the cells were growing well, with a large population of cells observed on the surface of the devices (**Figure 6**a), indicating low cytotoxicity of the tascPLA–OFETs. The MTT assay is widely used to quantify cytotoxicity in vitro. It is based on the reaction between 3-(4,5-dimethyl-thiazol-2-yl)-2,5-diphenyl-tetrazolium bromide (MTT) and mitochondrial succinate dehydrogenases in living cells to form a purple formazandye, which is insoluble in water but soluble in dimethyl sulfoxide. The colorimetric assay enables determination of the percentage of cells that remain viable after exposure conditions. Cytotoxicity of DNTT-tascPLA-OFETs was studied and the cells incubated with extracts from the DNTT-tascPLA-OFETs exhibited over 85% relative growth rations (RGR) (Figure 6b). More concentrated extracts or longer extraction time lead to a slightly lower RGR as expected. The good biocompatibility of the tascPLA–OFETs could be attributed to: i) tascPLA composing most of the OFETs already possesses good biocompatibility; ii) the organic semiconductors compose less than 0.1% total mass of the devices; iii) organic semiconductors are generally very insoluble in water, which is the medium for cell culture and living tissue.

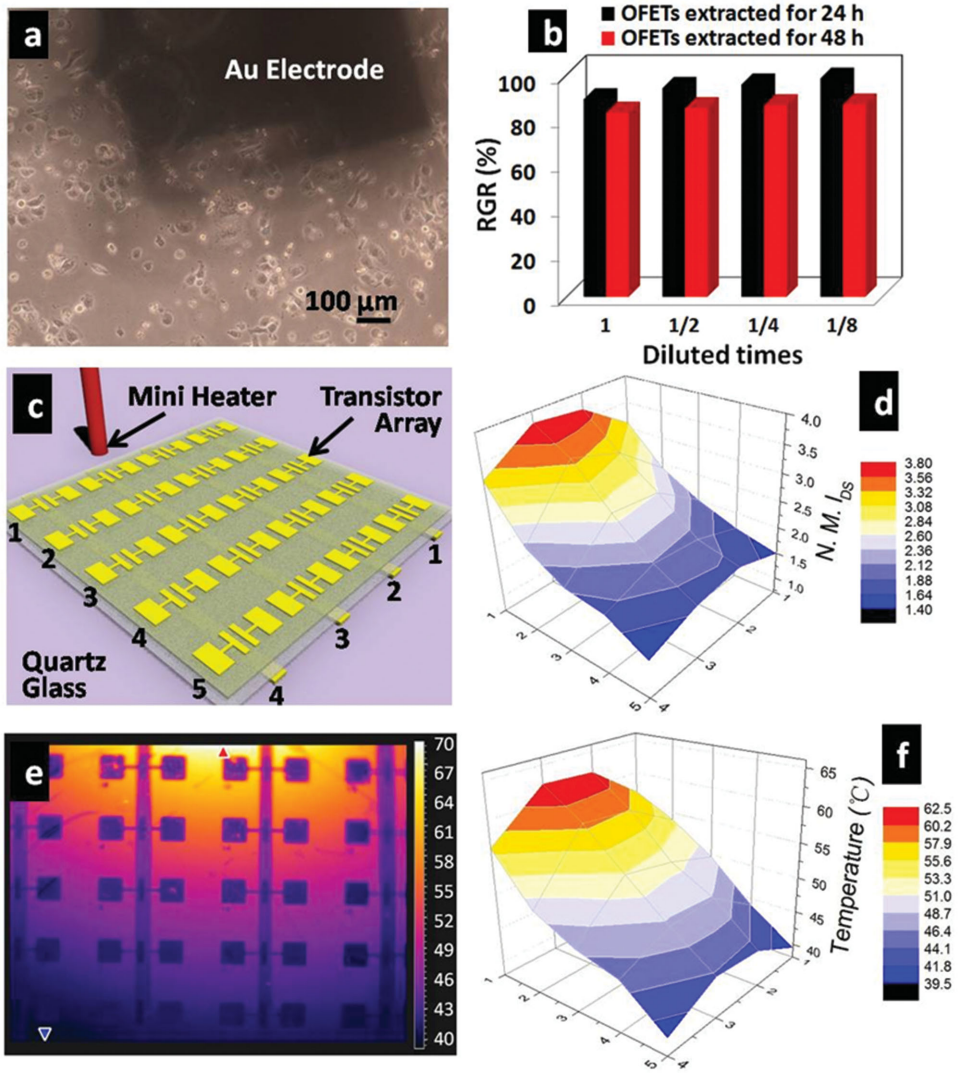

Figure 6. Biocompatibility and 2D temperature sensing of the OFET array for potential application for artificial skin: a) optical image of the 8_3-NTCDI-tascPLA-OFETs co-cultured with L929 cells, b) RGRs of cells incubated in the solutions containing extracted matters from the DNTT-tascPLA-OFETs, c) schematic presentation using the OFET array to detect a 2D temperature gradient field, d) the I_{DS} matrix output of the OFET array as a 2D temperature sensor, normalized to the initial I_{DS} matrix measured at room temperature, e) thermal infrared image of the OFET array on the gradient temperature field and f) the corresponding matrix temperature distribution extracted from the thermal infrared image.

2.5. Skin-Like Temperature Sensor Array

Due to their combined advantages, the tascPLA–OFETs are expected to be potentially applicable as an artificial skin with functional 2D temperature sensing.[21,33,39] Demonstration of such an application was realized by arranging the tascPLA–OFETs into a 2D array to detect a temperature gradient that was formed on a square of quartz glass heated by a thin copper rod (Figure 6c). The temperature distribution sensed by the artificial skin is exhibited in a matrix form of normalized I_{DS} of each OFET in the array (Figure 6d), displaying higher values at the locations closest to the heater rod and lower values at the regions spaced further away. The output results were further verified by employing thermal infrared imaging to detect the temperature field (Figure 6e). A 2D distribution of temperature in the same matrix form was extracted from the thermal infrared image at the same locations on the square (Figure 6f). The temperature distribution exhibited the same patterns as the aforesaid normalized I_{DS} distribution, which indicates our sensor array presents reliable 2D temperature detection.

3. Conclusion

In conclusion, biomaterial-based OFETs exhibit high thermal stability thanks to synthesizing and applying the tascPLA. Meanwhile, a simple strategy of fabricating OFET temperature sensors was proposed by utilizing the polar-group-induced MTR effect. The polar groups of the gate dielectric material enabled all the OFETs of the studied organic semiconductors to exhibit high-temperature sensitivity. Therefore, our OFETs made with tascPLA substrate/dielectric layers present many advantages including transparency, flexibility, thermal stability, high-temperature sensitivity, degradability, and biocompatibility, and

thus possess broad applicability for environmentally friendly electronics, implantable medical devices, etc. Furthermore, a 2D temperature field was successfully detected using an array of the fabricated tascPLA–OFETs. The reliable skin-like thermal sensitivity and the good biocompatibility thus make our OFETs potentially applicable for artificial skin.

4. Experimental Section

OFETs Fabrication and Characterization: Heavily n-type doped Si wafers with 300 nm of thermally grown SiO_2 layers were used as templates. Wafers were cleaned prior to use then surface modified with FOTS chloroform solution (1, v/v%) by spin coating at 3000 rpm for 20 s. Gold gate electrodes with thicknesses of 100 nm were thermally evaporated onto the Si templates through a shadow mask. PLA dielectric layers were then fabricated by two methods: i) 100 g L^{-1} PLA chloroform solution was spin coated at 3000 rpm for 60 s; ii) 50 g L^{-1} PLA chloroform solution was dip coated at a speed of 15 μm s^{-1}. More dilute solution and faster speed can result in a thinner film. Both samples were then annealed at 60 °C overnight in air. Thickness of the PLA dielectric layers was obtained by the following equation:

$$\text{Thickness} = \frac{\text{The mass of PLA film}}{\text{The area of PLA film} \times \text{density}}$$

While the mass was measured by a precision balance, the areas were obtained by measuring that of the Si templates, and the density of PLA is around 1.0 g cm^{-1}.[40] Organic semiconductor thin films at thicknesses of 100 nm were deposited by vacuum evaporation (0.2 Å s^{-1}, $P \approx 5 \times 10^{-4}$ Pa). Gold top contact source and drain electrodes with thicknesses of 100 nm were evaporated through a shadow mask with a spacing of $L = 1$ mm and $W = 30$ μm. Finally, OFETs were peeled off from the templates after the transistor fabrication was completed. OFETs with SiO_2 dielectric were fabricated by direct evaporation of organic semiconductors and gold electrodes onto the Si/SiO_2 wafers. Transistor measurements were carried out with a semiconductor parameter analyzer (Keithley 4200-SCS). Different measurement temperatures ranging from –25 °C to 200 °C were realized using a Lakeshore Co. Model 336. Flexible performance of the transistors was measured while the OFETs were tightly bent around cylinders with radii $r = 30$, 8, 4.5, 2.5, 1.2, and 0.8 mm, respectively.

Biocompatibility Measurements: Co-culture of L929 cells with the 8_3-NTCDI-tascPLA-OFETs was performed firstly by sterilization of the OFETs with ozone and ultraviolet light for 2 h. L929 cells at a concentration of 1×10^4 cells mL^{-1} were incubated with OFETs for 4 days while supplementing fresh medium every 6 h. Cell morphology was then observed using an inverted phase contrast microscope (IX71, OLYMPUS, Japan). Extracts of DNTT-tascPLA-OFETs and were obtained aseptically at 37 °C for 24 h or 48 h in 2.0 mL of RPMI1640. The extracts were then filtered, diluted to different concentrations in the range of 1 to 1/8 times of initial extracts, and finally mixed with 10% (v/v) calf serum for cell treatment. L929 cells at a concentration of 1×10^4 cells mL^{-1} were incubated with the aforesaid extracted solutions for 7 days while supplementing fresh medium every 24 h. For the negative control group, 100 μL of L929 cells were incubated using only fresh medium. Finally, 5 mg mL^{-1} MTT solution was added and cultured for 3.5 h. The formed precipitates were then filtered and dissolved in dimethylsulfoxide. The optical density (O.D.) value of each sample was measured using a microplate reader (Perlong, China) at 570 nm. RGR was calculated by using the following equation:

$$\text{RGR}(\%) = \frac{\text{The average O.D. of the test group}}{\text{The average O.D. of the negative control group}} \times 100\%$$

Skin-Like Temperature Sensing: A heating rod with a radius of 2 mm was vertically placed on a 4 cm × 4 cm quartz glass square, and the end face of the rod was closely contacted to the square (Figure 4c). A 2D temperature gradient field was thus formed on the square when balance was achieved between heat conducted from the hot rod and thermal diffusion and radiation on the quartz glass. A thermal infrared imager (FLIR SC300, with a close-up-lens 2×) was employed to detect the temperature distribution on the square. A 5 × 4 OFETs array was then placed on the square and the electric performance of each OFET was measured using a Keithley 4200-SCS. Normalized I_{DS} of the OFETs was obtained by dividing the I_{DS} of each OFET on the heated square by that at room temperature ($V_{DS} = -60$ V, $V_{GS} = -60$ V).

Supporting Information

Supporting Information is available from the Wiley Online Library or from the author.

Acknowledgements

The authors thank Prof. Howard E. Katz for discussions of the manuscript. This work was supported by the National Nature Science Foundation of China (Grant Nos. 51373123 and 21302142), Science & Technology Foundation of Shanghai (13PJ1408000 and 14JC1492600), and the 1000 youth talent plan. Z.F. acknowledges the National Nature Science Foundation of China (Grant Nos. 51373041). X.W. acknowledges the financial support from Science & Technology Foundation of Shanghai (14YF1403700).

Received: December 22, 2014
Revised: January 30, 2015
Published online: February 20, 2015

[1] C. J. Bettinger, Z. Bao, *Adv. Mater.* **2010**, *22*, 651.
[2] M. Irimia-Vladu, P. A. Troshin, M. Reisinger, L. Shmygleva, Y. Kanbur, G. Schwabegger, M. Bodea, R. Schwödiauer, A. Mumyatov, J. W. Fergus, V. F. Razumov, H. Sitter, N. S. Sariciftci, S. Bauer, *Adv. Funct. Mater.* **2010**, *20*, 4069.
[3] A. Campana, T. Cramer, P. Greco, G. Foschi, M. Murgia, F. Biscarini, *Appl. Phys. Lett.* **2013**, *103*, 073302.
[4] S.-W. Hwang, H. Tao, D.-H. Kim, H. Cheng, J.-K. Song, E. Rill, M. A. Brenckle, B. Panilaitis, S. M. Won, Y.-S. Kim, Y. M. Song, K. J. Yu, A. Ameen, R. Li, Y. Su, M. Yang, D. L. Kaplan, M. R. Zakin, M. J. Slepian, Y. Huang, F. G. Omenetto, J. A. Rogers, *Science* **2012**, *337*, 1640.
[5] S.-W. Hwang, J.-K. Song, X. Huang, H. Cheng, S.-K. Kang, B. H. Kim, J.-H. Kim, S. Yu, Y. Huang, J. A. Rogers, *Adv. Mater.* **2014**, *26*, 3905.
[6] M. Irimia-Vladu, *Chem. Soc. Rev.* **2014**, *43*, 588.
[7] J. Huang, H. Zhu, Y. Chen, C. Preston, K. Rohrbach, J. Cumings, L. Hu, *ACS Nano* **2013**, *7*, 2106.
[8] B. Jeong, Y. H. Bae, D. S. Lee, S. W. Kim, *Nature* **1997**, *388*, 860.
[9] X. Wu, A. E. Ghzaoui, S. Li, *Langmuir* **2011**, *27*, 8000.
[10] X. Wu, S. Li, F. Coumes, V. Darcos, J. Lai Kee Him, P. Bron, *Nanoscale* **2013**, *5*, 9010.
[11] A. Ignatius, L. E. Claes, *Biomaterials* **1996**, *17*, 831.
[12] J. Huang, J. Sun, H. E. Katz, *Adv. Mater.* **2008**, *20*, 2567.
[13] X. Liu, Y. Guo, Y. Ma, H. Chen, Z. Mao, H. Wang, G. Yu, Y. Liu, *Adv. Mater.* **2014**, *26*, 3569.
[14] M. E. Roberts, A. N. Sokolov, Z. Bao, *J. Mater. Chem.* **2009**, *19*, 3351.
[15] B. Crone, A. Dodabalapur, A. Gelperin, L. Torsi, H. E. Katz, A. J. Lovinger, Z. Bao, *Appl. Phys. Lett.* **2001**, *78*, 2229.
[16] M. E. Roberts, S. C. B. Mannsfeld, N. Queraltó, C. Reese, J. Locklin, W. Knoll, Z. Bao, *Proc. Natl. Acad. Sci. U.S.A.* **2008**, *105*, 12134.

[17] J. Huang, J. Miragliotta, A. Becknell, H. E. Katz, *J. Am. Chem. Soc.* **2007**, *129*, 9366.
[18] G. Schwartz, B. C. K. Tee, J. Mei, A. L. Appleton, D. H. Kim, H. Wang, Z. Bao, *Nat. Commun.* **2013**, *4*, 1859.
[19] D. J. Lipomi, M. Vosgueritchian, B. C. K. Tee, S. L. Hellstrom, J. A. Lee, C. H. Fox, Z. Bao, *Nat. Nanotechnol.* **2011**, *6*, 788.
[20] V. Podzorov, E. Menard, A. Borissov, V. Kiryukhin, J. A. Rogers, M. E. Gershenson, *Phys. Rev. Lett.* **2004**, *93*, 086602.
[21] T. Sakanoue, H. Sirringhaus, *Nat. Mater.* **2010**, *9*, 736.
[22] B. J. Jung, K. Lee, J. Sun, A. G. Andreou, H. E. Katz, *Adv. Funct. Mater.* **2010**, *20*, 2930.
[23] T. Yamamoto, K. Takimiya, *J. Am. Chem. Soc.* **2007**, *129*, 2224.
[24] K. Madhavan Nampoothiri, N. R. Nair, R. P. John, *Bioresour. Technol.* **2010**, *101*, 8493.
[25] R. E. Drumright, P. R. Gruber, D. E. Henton, *Adv. Mater.* **2000**, *12*, 1841.
[26] M. Kakuta, M. Hirata, Y. Kimura, *J. Macromol. Sci.Polym. Rev.* **2009**, *49*, 107.
[27] J. Shao, J. Sun, X. Bian, Y. Cui, G. Li, X. Chen, *J. Phys. Chem. B* **2012**, *116*, 9983.
[28] Y. Ma, W. Li, L. Li, Z. Fan, S. Li, *Eur. Polym. J.* **2014**, *55*, 27.
[29] B. Xu, D. Chen, R. C. Hayward, *Adv. Mater.* **2014**, *26*, 4381.
[30] M. Kaltenbrunner, T. Sekitani, J. Reeder, T. Yokota, K. Kuribara, T. Tokuhara, M. Drack, R. Schwödiauer, I. Graz, S. Bauer-Gogonea, *Nature* **2013**, *499*, 458.
[31] T. Sekitani, U. Zschieschang, H. Klauk, T. Someya, *Nat. Mater.* **2010**, *9*, 1015.
[32] H. T. Yi, M. M. Payne, J. E. Anthony, V. Podzorov, *Nat. Commun.* **2012**, *3*, 1259.
[33] T. Someya, Y. Kato, T. Sekitani, S. Iba, Y. Noguchi, Y. Murase, H. Kawaguchi, T. Sakurai, *Proc. Natl. Acad. Sci. U.S.A.* **2005**, *102*, 12321.
[34] G. Horowitz, *J. Mater. Res.* **2004**, *19*, 1946.
[35] V. Podzorov, M. E. Gershenson, *Phys. Rev. Lett.* **2005**, *95*, 016602.
[36] M. F. Calhoun, C. Hsieh, V. Podzorov, *Phys. Rev. Lett.* **2007**, *98*, 096402.
[37] V. Coropceanu, J. Cornil, D. A. da Silva Filho, Y. Olivier, R. Silbey, J.-L. Bredas, *ChemInform* **2007**, *107*, 926.
[38] D. D. Ateh, P. Vadgama, H. A. Navsaria, *Tissue Eng.* **2006**, *12*, 645.
[39] T. Someya, T. Sekitani, S. Iba, Y. Kato, H. Kawaguchi, T. Sakurai, *Proc. Natl. Acad. Sci. U.S.A.* **2004**, *101*, 9966.
[40] R. Auras, B. Harte, S. Selke, *Macromol. Biosci.* **2004**, *4*, 835.